CrossMark

ORIGINAL PAPER

Polyaniline-functionalized magnetic graphene oxide for dispersive solid-phase extraction of Cr(VI) from environmental waters followed by graphite furnace atomic absorption spectrometry

Shahram Seidi[1] · Mahshid Majd[1]

Abstract The present work describes synthesis of polyaniline-coated magnetic graphene oxide (MGO@PANI) as an efficient anion-exchange sorbent for dispersive magnetic solid-phase extraction of Cr(IV) from environmental samples. Graphite furnace atomic absorption spectrometry was used for analysis of the extracts. Synthesized nanoparticles were characterized by Fourier transform infrared spectroscopy, scanning electron microscopy and energy-dispersive X-ray analyzer. The important variables on the performance of the method such as pH of sample solution, sorbent amount, extraction and desorption time and type, concentration and volume of desorption elution were thoroughly optimized by means of experimental design and response surface methodology. Under the optimized condition, an aliquot of 50 mL of sample (pH 5.6) was extracted using 40 mg of MGO@PANI nanoparticles during 20 min. Then, the sorbent was desorbed using 850 μL of 2.75 mol L^{-1} H_2SO_4 under fierce vortex for 4.0 min. A preconcentration factor of 40 and an extraction recovery of 68% were provided by the proposed method. The limit of detection (3S/N) and quantification were obtained as 5.0 and 15 ng L^{-1}, respectively. The method showed a good linearity in the range of 15–300 ng L^{-1} with determination coefficient of 0.9987. The intra-day precision and inter-day precision (RSD%) were 5.3 and 8.2%, respectively. Finally, different water samples were examined by the proposed method to indicate its real applicability and the results showed good relative recoveries in the range of 100–110%.

✉ Shahram Seidi
  s.seidi@kntu.ac.ir

[1] Department of Analytical Chemistry, Faculty of Chemistry, K.N. Toosi University of Technology, P.O. Box 16315-1618, Tehran, Iran

 Springer

Graphical Abstract

Introduction

Environmental pollutants, especially heavy metals, are now the global warning giving threats to humanity. Chromium is one of the most common toxic ions contained in industrial waste water. Chromium salts are often used to manufacture leather products, paint, cement and anticorrosives [1, 2]. As a consequence, they can enter the environment from the discharge of steel, electroplating, tanning industries, etc. [3]. Chromium may also enter the tap-water supply from the corrosion inhibitors used in water pipes and containers.

It is found that chromium is a highly toxic metal element for microorganisms and plants. The entrance of chromium into the environment affects the growth of plants and metabolic functions of the living species [4]. Moreover, chromium has been reported as a carcinogenic agent in lung cancer [5]. The most prominent example of toxic chromium is hexavalent chromium. The toxicity of Cr(VI) is due to its strong oxidational properties and easy permeation of biological membranes [6]. World health organization (WHO) establishes a maximum amount of total chromium in drinking water as being 0.05 mg L^{-1}, while in Japan, maximum tolerable values for waste water are 0.5 and 0.05 mg L^{-1} for total chromium and Cr(VI), respectively [7]. Therefore, the accurate trace determination of these heavy metals is of vital importance. However, low concentration and matrix interferences restrict direct determination of metal ions at trace levels. These limitations make it necessary to use a suitable sample preparation method for preconcentration of trace elements and providing sample cleanup.

The most widely used techniques for separation/preconcentration of chromium include cloud point extraction (CPE) [8], membrane extraction (ME) [9], liquid-phase microextraction [10–12], solid-phase extraction (SPE) [13–15], co-precipitation [16] and ion-exchange separation [17]. Among these techniques, SPE is a popular technique due to its good reproducibility, simplicity and high selectivity and preconcentration factors [18].

However, limitations such as cartridge blockage and being time-consuming for analysis of samples with large volumes lead to introducing a new solid-based extraction technique called as dispersive solid-phase extraction (DSPE). DSPE is based on dispersion of the solid sorbents in the whole of sample solution and their collection using centrifugation (non-magnetic sorbents) or applying an external magnetic field (magnetic sorbents). Then, the extracted analytes are eluted using a suitable desorption solvent and analyzed. The key point for an efficient and selective extraction by DSPE is the applied sorbent. The introduction of nanomaterials has prompted the development of flexible nanocomposites and consequently been emerged as a subject of enormous scientific interest in DSPE. This fact can be attributed to the high surface area and the tunable surface functionalization possibility of the nanomaterials.

More recently, the current research activities have been evolved toward graphene–polymer nanocomposites due to

the outstanding structural performance and the multifunctional properties provided by the synergistical combination of the characteristics of both components. Among the different types of polymers, conductive polymers as multifunctional materials have attracted much attention. Most conductive polymers are prepared by oxidative coupling of monocyclic precursors. Polyaniline (PANI), as one of the most promising conducting polymers, has drawn more attention due to its high electrical conductivity, excellent environmental stability, relatively low density and low cost as well as easy and facile synthesis. PANI can be found in three oxidation states, including leucoemeraldine (white/clear and colorless), emeraldine (green for the emeraldine salt, blue for the emeraldine base) and pernigraniline (blue/violet) [19]. The most useful form of PANI is emeraldine base attributing to its high stability at room temperature and the fact that its conductivity can be tuned by adjusting the level of doping acid. This versatility has made PANI attractive for many applications such as sensors and anticorrosion coatings [19]. Moreover, it seems that this tune ability makes it possible to use PANI in the form of emeraldine salt as an efficient alternative anion-exchange sorbent for DSPE [20].

The aim of this work is to prepare MGO@PANI and its application as an anion-exchange nanocomposite for rapid and selective extraction of Cr(VI) ions. The final extracted phase was ultimately analyzed via graphite furnace atomic absorption spectrometry (GFAAS). A central composite design (CCD) was used for the optimization of extraction parameters. The developed method was successfully applied for ultratrace determination of chromium in different wastewater samples.

Experimental

Apparatus

A GBC 932 plus atomic absorption spectrometer (GBC Scientific Equipment, Australia) equipped with a GF-3000 graphite furnace atomizer and a PAL-3000 autosampler was used in this study. A chromium hollow cathode lamp was used as a radiation source for absorbance measurements at a wavelength of 357.9 nm. Also, a deuterium lamp was used for background correction. Pure Ar (99.999%) was used as carrier gas. Pyrolytically coated graphite tubes were used for analysis. The instrument was operated under the conditions recommended by the manufacture (slit width: 0.2 nm and the lamp current: 0.5 mA). The graphite furnace temperature program for the determination of chromium is shown in Table 1. A mixture of palladium (1000 mg L^{-1} $PdCl_2$) and ascorbic acid (1% w/v) was used as chemical modifier during GFAAS analysis for the more

Table 1 Graphite furnace operating conditions for determination of Cr(VI)

Step	Temperature (°C)	Ramp (s)	Time (s)	Gas flow (L min^{-1})
Drying				
1	50	1	2	2.5
2	90	10	15	2.5
3	120	15	10	2.5
Ashing				
4	700	10	5	2.5
5	700	0	1	0
Atomization				
6	1800	0.7	2	0
Cleaning				
7	2000	1	2	2.5

efficient removal of the matrix constituent during the ashing step and guarantee of analyte retention until the atomization step [21]. Measurements were taken in the peak area mode. A Metrohm 827 pH meter (Herisau, Switzerland) equipped with a combined glass calomel electrode was used for pH adjustment. Ultrapure water was prepared by a Younglin 370 series aqua MAX purification instrument (Kyunggi-do, Korea).

Reagents and materials

All used chemicals were of analytical reagent grade. Ethanol (EtOH, 96%), hydrochloric acid (37%), sulfuric acid (98%), orthophosphoric acid (85%), potassium dichromate, potassium permanganate ($KMNO_4$, 99%), iron(III) chloride hexahydrate ($FeCl_3 \cdot 6H_2O$, 99%), iron(II) tetrahydrate ($FeCl_2 \cdot 4H_2O$), aniline, sodium persulfate ($Na_2S_2O_4$), ammonium acetate, natural graphite and cetyltrimethylammonium bromide (CTAB) were purchased from Merck (Darmstadt, Germany). A stock solution (1000 mg L^{-1}) of Cr(VI) was prepared by dissolving appropriate amounts of potassium dichromate in ultrapure water. Working standard solutions were prepared daily through dilution of the stock solution.

Synthesis of graphene oxide

Graphene oxide (GO) was synthesized by a modified Hummers method [22]. Briefly, 360 mL of H_2SO_4 and 40 mL of H_3PO_4 were cooled by immersing the mixture in an ice bath and then 3.0 g of graphite was added. The mixture was stirred by a magnetic stirrer during the process. Then, 18.0 g of $KMnO_4$ was gradually added. The solution was stirred for about 24 h until the solution color was changed to brown. Then, the solution vessel was immersed in an ice bath and 400 mL of iced deionized water was added. The solution color was changed to dark red. Afterward, 150 mL

of H_2O_2 (30%) was added to the solution and the mixture color was changed to orange. The final solution was centrifuged and the precipitate (GO) was washed two times with water and ethanol and dried at 65 °C in an electric constant temperature drying oven (Fan Azma Gostar, Iran).

Synthesis of magnetic graphene oxide

Magnetic graphene oxide (MGO) was prepared through the chemical co-precipitation of Fe(III) and F(II) ions in the presence of graphene oxide. One gram of GO was added to 50 mL of deionized water and dispersed for about 1 h using an ultrasonic bath (Bandelin, Germany). The mixture was heated up to 80 °C, and then, 8.4 g $FeCl_3 \cdot 6(H_2O)$ and 2.25 g $FeCl_2 \cdot 4(H_2O)$ were added in the mixture under purging of N_2 gas. After 15-min stirring, 20 mL ammonia (25%) was added and black precipitates were instantly formed. The precipitates were collected by a 1.4-T magnet (2 cm × 4 cm × 5 cm) and washed with distilled water and ethanol and dried at 65 °C in the oven.

Synthesis of MGO@polyaniline

A schematic presentation of the sorbent is presented in Fig. 1. For this purpose, 3.0 g of MGO together with

0.5 g of CTAB was sonicated in 150 mL of deionized water for 15 min. Dispersed MGO was transferred into a double-walled glass vessel, and the system was connected to a circulating temperature controller (Optima Tokyo, 740, Japan). The mixture temperature was adjusted at 5 °C. After gradual addition of 6.0 mL aniline, a solution of 9.0 g sodium persulfate in 10 mL distilled water was dropwise added to the mixture as an oxidant. The mixture was stirred about 5 h using a mechanical stirrer. Finally, the magnetic precipitates were collected by the magnet, washed with HNO_3 1.0 mol L^{-1}, ethanol and ultrapure water and dried at 65 °C in oven.

Synthesis of Fe₃O₄@polyaniline

Fe_3O_4@PANI was synthesized using the same procedure used for MGO@PANI to compare the extraction efficiency of both sorbents. First, Fe_3O_4 nanoparticles were synthesized by the similar process used for the synthesis of MGO, except addition of GO. Next, 3.0 g of Fe_3O_4 together with 0.5 g of CTAB was sonicated in 150 mL of deionized water for 15 min and exposed to the same synthesis procedure performed for Fe_3O_4@PANI.
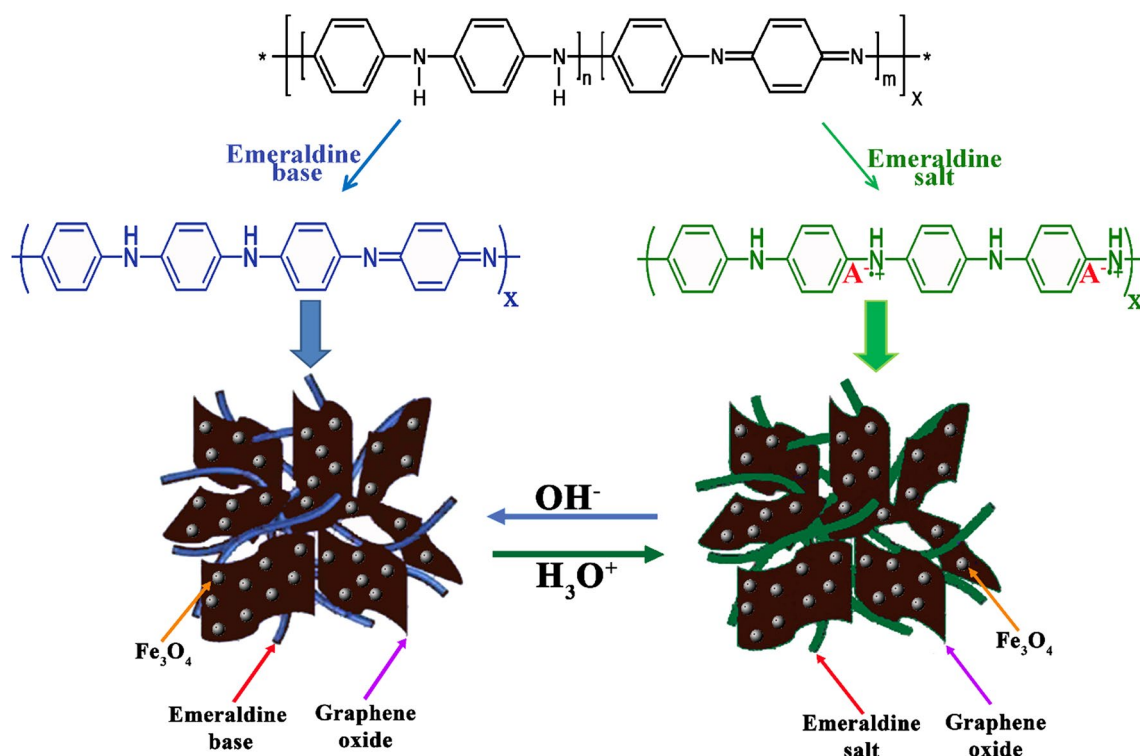

Fig. 1 Schematic presentation of MGO@PANI and reversible conversion of emeraldine base (EB) to emeraldine salt (ES) by doping with a protonic acid and its dedoped back via deprotonation using a base

Dispersive solid-phase extraction procedure

A schematic of the extraction procedure is presented in Fig. 2. Forty milligrams of the solid sorbent was added into 50 mL of sample solution (5.0 mmol L^{-1} ammonium acetate, pH 5.6) containing target ions. The mixture was sonicated for 10 s and stirred about 20 min. Then, the sorbent was collected by the magnet and the supernatant was discarded. As desorbing eluent, 850 µL of H_2SO_4 2.75 mol L^{-1} was added. The mixture was transferred into a conical-bottom centrifuge tube and agitated by a vortex (IKA, model MS3 basic) for 4.0 min. The sorbent was separated from the eluent by the magnet. Then, the collected eluent was passed through a disposable 0.22-µm cellulose acetate filter and introduced into the furnace for further analysis.

Experimental design

In the present work, a central composite design (CCD) was applied to optimize the experimental factors of both adsorption and desorption steps consisting of sorbent amounts, sample pH, adsorption and desorption times as well as concentration and volume of acidic eluent. All optimizations were carried out in ultrapure water spiked with Cr(VI) at the concentration of 100 ng L^{-1}. A Design-Expert 8.0.6 trial version (Stat-Ease Inc., MN, USA) software package was used for the design generation and statistical analysis.

Results and discussion

Characterization of MGO@PANI

Fourier transform infrared (FT-IR) spectra (4000–200 cm^{-1}) in KBr were recorded using Bruker IFS 66/S FT-IR spectrometer (Bruker Company, Germany). Figure 3 shows the spectra of GO, MGO and MGO@PANI nanoparticles. In Fig. 3a, the broad band around 3430 cm^{-1} is characteristic of the stretching vibration of OH group and the peaks at 1744, 1051 and 857 cm^{-1} show the C=O, C–O and epoxy stretching vibrations, respectively. Also, the broad band around 3430 cm^{-1} in Fig. 3b is related to the stretching vibration of OH group and peaks at 619 and 590 cm^{-1} belong to the stretching vibration of Fe–O–Fe. The band around 3461 cm^{-1} in Fig. 3c is characteristic of the stretching vibration of NH_2, and peaks at 755 and 1583 cm^{-1} are for the N–H wagging vibration and the N–H bending, respectively. Peaks at 1142 and 1237 cm^{-1} are attributed to the C–N stretching vibration, and peak at 1300 cm^{-1} is for the aromatic C–N stretching vibration. A peak at 2930 cm^{-1} is also for the stretching vibration of C–CH_2 (the methylene chain of CTAB).

The adsorption characteristics of materials are related to their physical morphology. Thus, the surface morphology of MGO@PANI is an important factor affecting its performance. The morphological structure of MGO was characterized by a scanning electron microscope (SEM) model EM3200 from KYKY Zhongguancun (Beijing, China).

Figure 4a shows the sheet-like structure of the MGO, and Fig. 4b indicates different surface morphology and the existence of some bead-like particles which are the evidences of PANI attachment on MGO. Such physical morphology of PANI@MGO may significantly increase the available surface area of PANI@MGO and therefore enhance the extraction efficiency.

The energy-dispersive X-ray (EDX) spectrometry analysis of the nanocomposite was performed using a Tescan Vega diffractometer (Brno, Czech Republic). Elemental analysis in Fig. 4c shows the presence of 2.17% N in the structure of magnetic sorbent which indicates that MGO
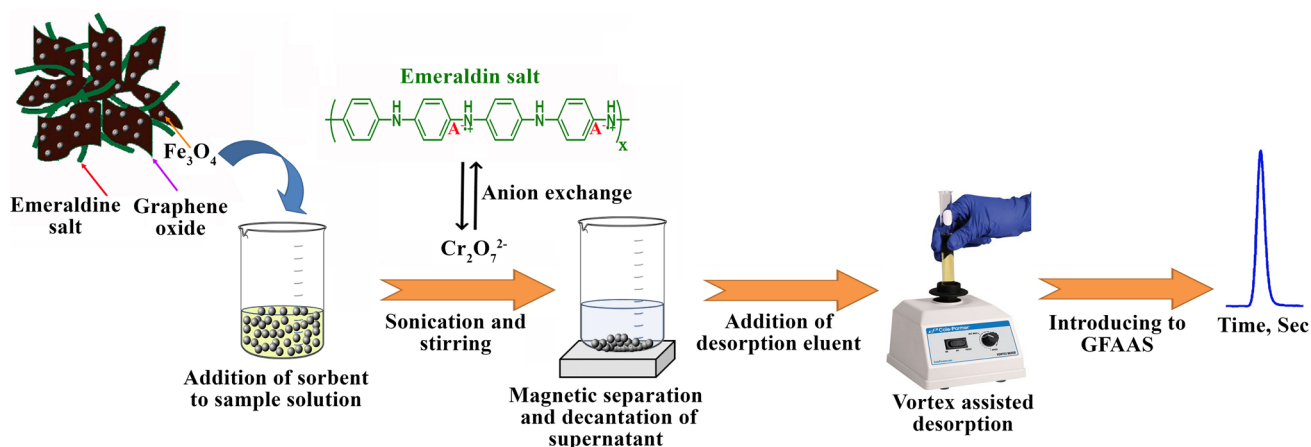

Fig. 2 Representation of dispersive magnetic solid-phase extraction (DMSPE) procedure

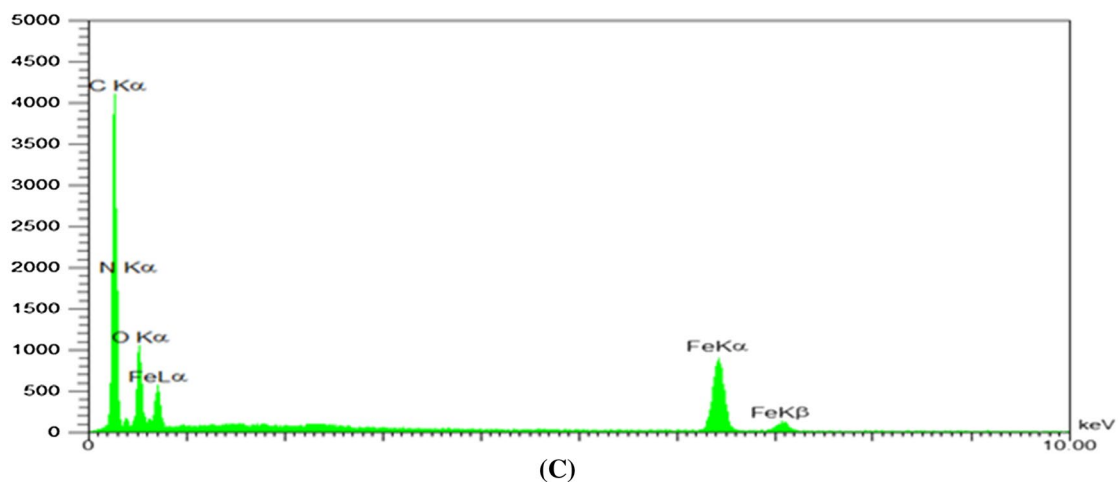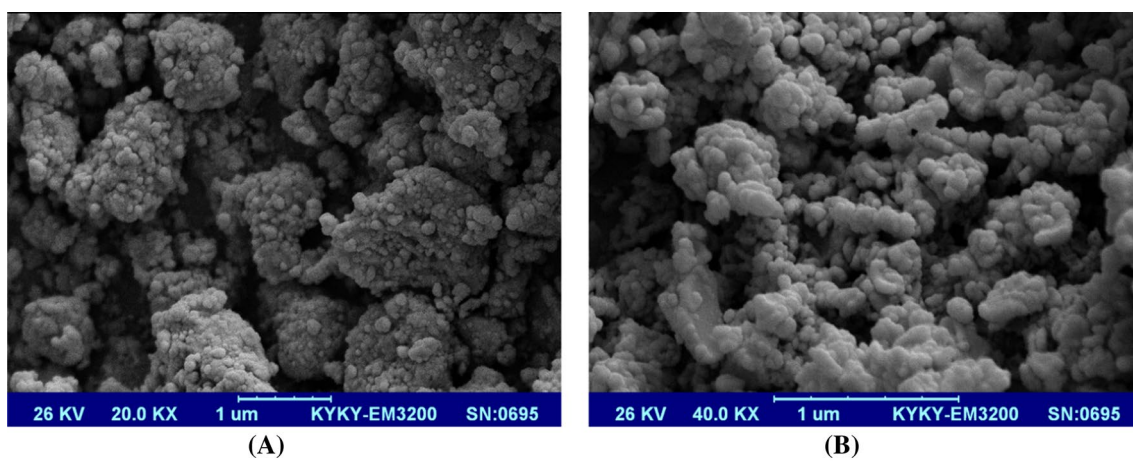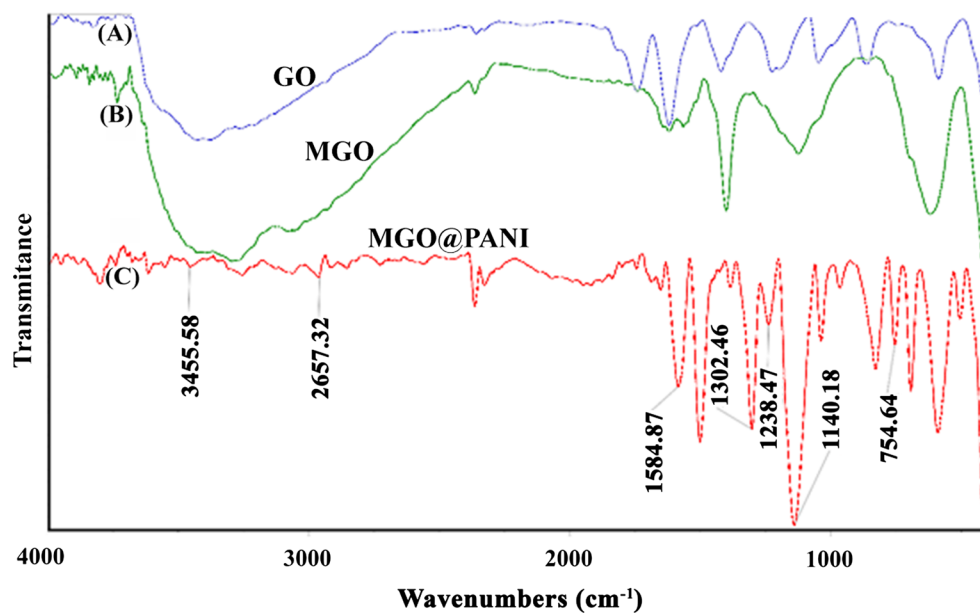**Fig. 3** FT-IR spectra of GO, MGO and MGO@PANI

Fig. 4 Scanning electron microscopy (SEM) images of **a** MGO and **b** MGO@PANI and **c** energy-dispersive X-ray (EDX) spectrum of MGO@PANI back to EB via deprotonation at the presence of a base (Fig. 1)

nanoparticles are beneficially modified with PANI (C: 27.20%, Fe: 66.03%, O: 4.60%, N: 2.17).

Optimization procedure

A central composite design (CCD) was selected for the optimization of parameters affecting adsorption and desorption steps of DMSPE procedure. CCD is a second-order model which permits accurate description of the response behavior with the variation of nonlinear factors. CCD consists of factorial points ($N_f = 2^f$), star or axial points ($N_a = 2f$) and center points (N_0). The total number of design points needed (N) is determined by the following equation:

$$N = 2^f + 2f + N_0 \tag{1}$$

Depending on the value of star point (α) calculating by the following equation, CCD includes different types such as orthogonal central composite design (OCCD) in which $|\alpha| > 1$.

$$\alpha^2 = \frac{\sqrt{(N_f + N_a + N_0)N_f} - N_f}{2} \tag{2}$$

In this study, OCCD was used to optimize the experimental parameters influencing the extraction efficiency of chromium. The key variables selected for both adsorption and desorption steps as well as their levels are shown in Table 2. To estimate the overall error, five additional experiments were carried out at the center point. According to Eq. 1, the experimental design required 19 experiments which were performed in random order to minimize the effects of bias

errors on the measurements. Considering Eq. (2), the needed value for α to ensure the orthogonality was ± 1.4712.

For an experimental design with three factors, the model including linear, quadratic and cross-terms can be expressed as the following equation:

$$\begin{aligned} \text{Response} = {}& a_0 + a_1F_1 + a_2F_2 + a_3F_3 + a_4F_1F_2 + a_5F_1F_3 \\ & + a_6F_2F_3 + a_7F_1^2 + a_8F_2^2 + a_9F_3^2 \end{aligned} \tag{3}$$

in which F_1–F_3 are experimental factors, and a_0–a_9 are the coefficient values obtained through multiple linear regression. Adjusted coefficient of determination (Adj R^2) and lack of fit (LOF) are used to express the fit quality of a polynomial model equation.

Analysis of variance (ANOVA) was used to evaluate the models at 95% confidence level (p value 0.05). ANOVA results for the adsorption step are shown in Table 3. A p value <0.05 indicates the statistical significance of each model as well as the investigated parameters. Obtained model for the adsorption steps is summarized in Table 2. Statistical analysis revealed that the model was fitted accurately to the experimental data.

After ascertaining the validity of the model, response surface methodology (RSM) was applied to illustrate relationships between parameters and responses. The quadratic response surface for three factors generates a four-dimensional plot; thus, to visualize the response versus variables, one variable was held constant at its optimum and the response variation is mapped against two other variables. Also, two-dimensional contour plots on the basis of the model equations were shown below the response surfaces,

Table 2 Experimental factors, levels, statistical adsorption/desorption models and their evaluating parameters using OCCD for determination of chromium by the proposed extraction procedure

Step	Factors	Symbol	Levels				
			$-\alpha$	-1	0	$+1$	$+\alpha$
Adsorption step	pH	X_1	2.31	3.5	5	7.25	8.19
	Extraction time (min)	X_2	13.18	20	30	40	46.82
	Adsorbent amount (mg)	X_3	13.18	20	30	40	46.82
Desorption step	Acid concentration (mol L^{-1})	Y_1	0.9	1.25	2	2.75	3.1
	Desorption time (min)	Y_2	1.53	2	3	4	4.47
	Desorption volume (µL)	Y_3	479.32	550	700	850	920.68

Model description	Adsorption model	Desorption model
Model equation	Peak area $= -0.05324 + 0.03653 \times X_1 - 0.00444 \times X_2 + 0.00458 \times X_3 + 0.000323 \times X_1X_2 - 0.0000553 \times X_2X_3 - 0.00382 \times X_1^2 + 0.0000727 \times X_2^2$	Peak area $= +1.05973 - 0.26797 \times Y_1 - 0.35634 \times Y_2 - 0.000284 \times Y_3 + 0.077167 \times Y_1Y_2 + 0.0000989 \times Y_1Y_3 + 0.000273 \times Y_2Y_3 - 0.000000539 \times Y_3^2$
Adj R^2	0.9465	0.9304
Model p value	<0.0001 (significant)	<0.0001 (significant)
LOF p value	0.8540 (not significant)	0.0669 (not significant)

Table 3 Analysis of variance (ANOVA) of the quadratic model for the adsorption step

Source	Sum of squares	df	Mean square	F value	p value Prob. > F	
Model	0.017	9	0.00187	44.96	<0.0001	Significant
pH (X_1)	0.00154	1	0.00154	36.93	0.0002	Significant
Extraction time (X_2)	0.00000238	1	0.00000238	0.057	0.8167	Not significant
Adsorbent amount (X_3)	0.012	1	0.012	279.08	<0.0001	Significant
$X_1 X_2$	0.000255	1	0.000255	6.12	0.0354	Significant
$X_1 X_3$	0.000000491	1	0.000000491	0.012	0.9159	Not significant
$X_2 X_3$	0.000244	1	0.000244	5.86	0.0386	Significant
X_1^2	0.00170	1	0.00170	40.8	0.0001	Significant
X_2^2	0.000833	1	0.000833	19.99	0.0016	Significant
X_3^2	0.000188	1	0.000188	4.52	0.0624	Not significant
Residual	0.000375	9	0.0000417			
Lack of fit	0.000116	5	0.0000233	0.36	0.854	Not significant
Pure error	0.000259	4	0.0000647			
Cor. total	0.017	18				

which display the interactions between the independent variables and assist in determining the optimal operating conditions for desirable responses.

Figure 5a, b illustrates the effects of experimental factors on the adsorption steps. The pH of sample solution has significant effects on (1) the chemical characteristics of MGO@PANI and (2) the dominant form of Cr(VI) ions. PANI is known as a para-linked phenylene amine imine. The general formula of PANI is shown in Fig. 1 that in which m indicates the function of oxidized units. PANI is called leucoemeraldine when no oxidized unit exists in its structure ($m = 0$), whereas pernigraniline is referred to the fully oxidized form of PANI ($m = 1$). The half-oxidized polymer ($n = m = 0.5$) is termed as the emeraldine base (EB). EB is considered as the most useful form of PANI because it not only has high room temperature stability, but also against the two other forms can be converted to a conductive polymer, named as emeraldine salt (ES), by doping with a wide variety of protonic acids (Fig. 1). In addition, ES can be dedoped. On the other hand, according to the literature, the dominant form of Cr(VI) at pH values in the range of 5–6.5 and concentrations lower than 0.03 mol L^{-1} is $Cr_2O_7^{2-}$ [23]. This form is more favorable than CrO_4^{2-} or $HCrO_4^-$ because two moles of Cr(VI) are adsorbed by adsorption of each mole of $Cr_2O_7^{2-}$ ion resulted in the increase in extraction efficiency.

As can be seen in Fig. 5b, the best extraction efficiency was obtained at pH of 5.6. A high pH value may lead to conversion of ES to EB and consequently decreasing of anion-exchange ability of sorbent, conversion of the dominant form of Cr(IV) to the other forms as well as increasing of competition among OH$^-$ and $Cr_2O_7^{2-}$ ions for adsorption. Moreover, decreasing of adsorption efficiency at low pH values can be attributed to the variation of the dominant form of Cr(VI) and also increasing of competition among anions of acids and $Cr_2O_7^{2-}$ ions for anion exchange on the surface of sorbent.

Another influential parameter on the extraction efficiency is adsorbent amounts. This effect was studied by varying the amounts of the sorbent within the range of 13.18–46.82 mg (Fig. 5a). The results showed that 40 mg is sufficient for the quantitative recovery of the chromium ions. The lower sorbent dosage is not able to extract the maximum amounts of the target analyte. On the other hand, the extra amount of sorbent reduces the signal since a larger volume of desorbing eluent is needed for the complete washing of sorbent. DSPE is an equilibrium extraction method; thus, enough time is needed to reach the maximum extraction efficiency. According to the results in Fig. 5a, 20 min was selected as the optimum value for the next experiments.

To verify the proposed optimum adsorption conditions by the software, some practical experiments were carried out and the obtained response was compared by the predicted value. The predicted response by the software at the optimum conditions for the adsorption step was within the range of 0.13–0.16 at the confidence interval of 95%. The practical response was obtained as 0.151 ± 0.010 which was within the predicted range, confirming the proposed optimum adsorption conditions.

Type, volume and concentration of the desorbing eluent as well as desorption time are the main parameters affecting the desorption efficiency. The type of the desorbing eluent was investigated separately. This eluent should have fast kinetic and adequate affinity to the target analyte. To find a suitable desorbing solution, H_2SO_4, HNO_3 and HCl with the concentrations of 3.0 mol L^{-1} were examined. The results indicated no significant difference among the desorbing eluents. However, HCl is corrosive for graphite furnace [24], and H_2SO_4 provided a little better signal which
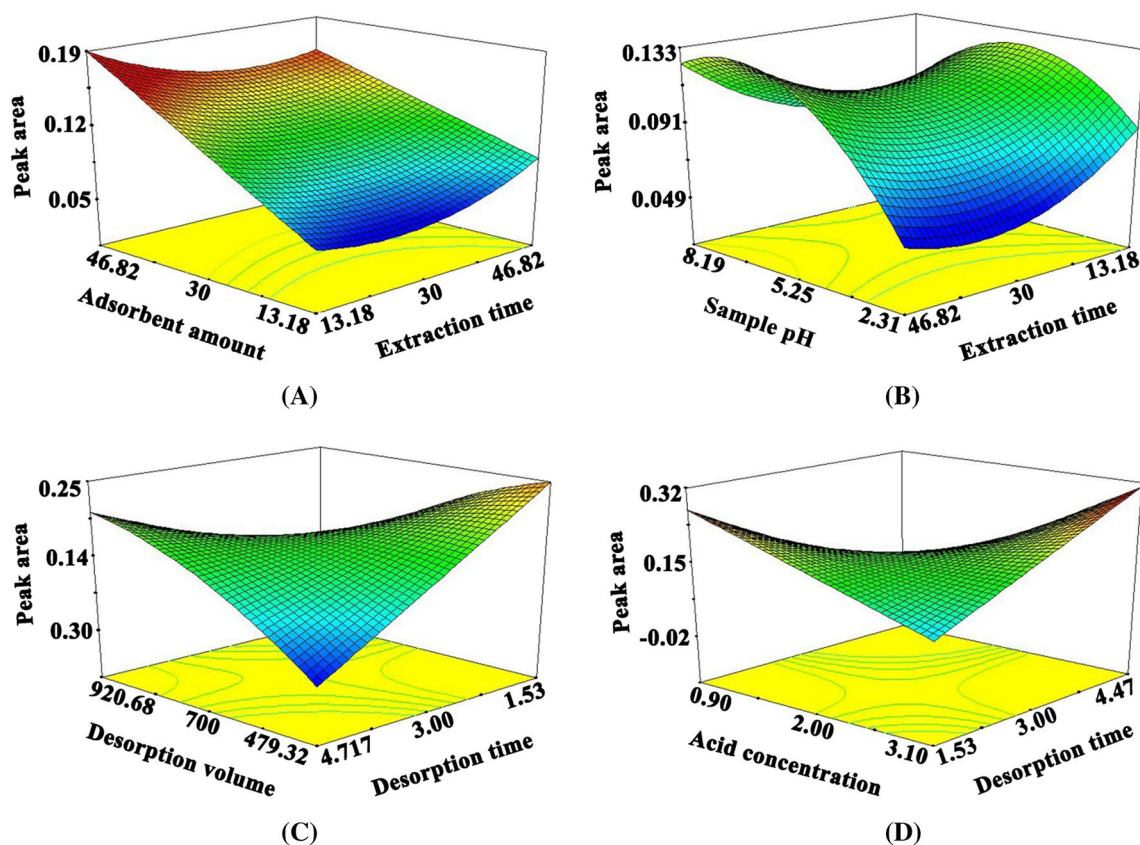
Fig. 5 Response surfaces along with the *contours plots* for optimization of adsorption (**a**, **b**) and desorption (**c**, **d**) steps illustrating the relationship among the experimental factors

may be due to more anion-exchange ability of SO_4^{2-}. Therefore, H_2SO_4 was selected as the best desorbing eluent for the rest of the experiments.

Three other variables were optimized using OCCD. ANOVA results of the desorption step are shown in Table 4. Obtained model for the adsorption steps is summarized in Table 2. The RSMs are shown in Fig. 5c, d. Increasing the eluent volume may decrease the preconcentration factor. However, an enough volume of the desorbing solvent is required for proper elution of the adsorbed analyte from the surface of the sorbent. The results indicated that 850 μL of 2.75 mol L^{-1} H_2SO_4 with a fierce vortex for 4.0 min was sufficient to gain the maximum recovery of Cr(VI) ions. The predicted response for the desorption step was within the range of 0.24–0.31 (confidence interval of 95%). The practical response (0.245 ± 0.012) for this step was also within the predicted range, indicating the suitability of the selected desorption conditions.

Analytical performance

Optimized conditions were performed to evaluate the figures of merit of the proposed method. The calibration curve was linear over the range of 15–300 ng L^{-1}. The equation of the extraction calibration curve was $A = 0.6881$ (± 0.0295) $C + 0.0110$ (± 0.0010), where A is the peak area and C is the concentration of analyte (μg L^{-1}), with the determination coefficient (R^2) of 0.9987. Also, the equation for direct calibration was $A = 0.0172$ (± 0.0011) $C + 0.0220$ (± 0.0013) with R^2 of 0.9996. The limit of detection (LOD) based on a signal-to-noise ratio (S/N) of 3 was 5.0 ng L^{-1}, and the low limit of quantification (LLOQ) was 15 ng L^{-1}. The preconcentration factor (PF), calculated as the ratio of the slopes of the calibration curves acquired by the proposed method and through the direct analysis of chromium by furnace, was found to be 40. The extraction recovery (ER%) was 68% which was defined as the percentage of the final moles of analyte in the desorbing eluent to the moles initially presented in the sample solution. The relative standard deviations (RSDs%) for the intra- and inter-assay precisions at the concentration of 100 ng L^{-1} were 5.3 and 8.2%, respectively.

A comparison of the present work with other dispersive solid-phase extraction techniques used for preconcentration of Cr(VI) from water samples is summarized in Table 5. It is obvious that the method is quite comparable

Table 4 Analysis of variance (ANOVA) of the quadratic model for the desorption step

Source	Sum of squares	df	Mean square	F value	p value Prob. > F	
Model	0.052	9	0.00583	35.27	<0.0001	Significant
Acid concentration (Y_1)	0.00744	1	0.00744	44.99	<0.0001	Significant
Desorption time (Y_2)	0.00156	1	0.00156	9.44	0.0133	Significant
Desorption volume (Y_3)	0.000144	1	0.000144	0.87	0.3744	Not significant
Y_1Y_2	0.027	1	0.027	162.08	<0.0001	Significant
Y_1Y_3	0.000990	1	0.000990	5.99	0.0369	Significant
Y_2Y_3	0.013	1	0.013	80.85	<0.0001	Significant
Y_1^2	0.000781	1	0.000781	4.72	0.0578	Not significant
Y_2^2	0.0000280	1	0.0000280	0.17	0.6905	Not significant
Y_3^2	0.000138	1	0.00138	8.33	0.018	Significant
Residual	0.00149	9	0.000165			
Lack of fit	0.00129	5	0.000258	5.24	0.0669	Not significant
Pure error	0.000197	4	0.0000493			
Cor. total	0.054	18				

Table 5 Comparison of the proposed method with other magnetic DSPE techniques for extraction of Cr(VI) from water samples

Sorbent[a]	PF	Sample volume (mL)	LOD (µg L^{-1})	RSD%	Linear range (µg L^{-1})	Detection technique[b]	References
Bismuthiol-II-immobilized MNPs	96	100	0.043	3.5	–	ICP-OES	[18]
Mesoporous amino-functionalized Fe_3O_4/SiO_2	16	45	3.2	<5.5	LOQ–100	FAAS	[25]
Fe_3O_4/Al_2O_3	120	250	1.4	3.4	10–1000	FAAS	[26]
Polyaniline-coated Fe_3O_4	300	100	0.1	<6.3	0.3–100	HPLC–UV	[27]
Triazine-functionalized Fe_3O_4	–	–	2	1.4	–	UV–Vis	[28]
MNPs coated with [HMIM]Br	112	40	0.003	–	0.01–0.5	GFAAS	[29]
Chitosan-modified MNPs	100	150	0.03	<5.6	0.1–100	ICP-OES	[30]
Zincon-immobilized silica-coated Fe_3O_4	150	100	0.016	6.2	–	GFAAS	[31]
TEPA-functionalized Fe_3O_4	125	250	0.16	1.9	–	GFAAS	[32]
Amine-functionalized Fe_3O_4	47	–	0.0021	4.5	0.05–100	ICP-MS	[33]
Decanoic acid-coated Fe_3O_4	120	47	0.5	2.8	1–400	ICP-OES	[34]
MGO@PANI	40	50	0.005	5.3	0.015–0.3	GFAAS	This work

[a] *MNPs* Magnetic nanoparticles, *[HMIM]Br*: 1-hexadecyl-3-methylimidazolium bromide, *TEPA* tetraethylenepentamine

[b] *ICP-OES* inductively coupled plasma-optical emission spectrometry, *FAAS* flame atomic absorption spectrometry, *HPLC–UV* high-performance liquid chromatography–ultraviolet detection, *GFAAS* graphite furnace atomic absorption spectrometry, *ICP-MS* inductively coupled plasma-mass spectrometry

in the cases of LOD, linearity and PF with other reported techniques. However, some reports benefited from high-tech and expensive instruments which are not available in all laboratories like ICP-MS offer lower LODs. Against the other used non-magnetic sorbents, the magnetic property of the synthesized sorbent in this work enabled easy collection of the sorbent after extraction, by applying an external magnetic field. Against some reported sorbents, MGO@PANI is provided by a simple and cost-effective procedure with minimum consumption of organic solvents. Moreover, the proposed MGO@PANI sorbent provided selective extraction of Cr(VI) in the presence of different cations due to the anion-exchange mechanism.

Sorbent capacity

The sorption capacity is defined as maximum amounts of the analyte which can be adsorbed by the certain amounts of a sorbent. This parameter was determined for both MGO@PANI and Fe_3O_4@PANI by dispersing 100 mg of each sorbent into 50 mL of 10 mg L^{-1} of solution, and the optimal conditions were performed for extraction of the

Table 6 Determination of Cr(VI) in different water samples using the MGO@PANI sorbent followed by GFAAS

Sample	Spiked (ng L^{-1})	Found $\pm$ SD^a (ng L^{-1})	Relative recovery%
Javanmardan river	0	ND^a	–
	50	54.0 $\pm$ 2.1	108.0
Ferdows river	0	ND	–
	50	50.7 $\pm$ 0.91	101.4
Tannery waste water	0	244.7 $\pm$ 12.7	–
	50	298.0 $\pm$ 10.6	106.7
Laboratory water	0	40.0 $\pm$ 2.5	–
	50	91.5 $\pm$ 5.0	103.0
Sattari St. river	0	ND	–
	50	52.0 $\pm$ 1.7	104.0

^{a} *SD* standard deviation ($n = 3$)

targets. The capacity was calculated through the differences in the initial and the final amounts of chromium ions in the solution. The sorption capacity of MGO@PANI and Fe$_3$O$_4$@PANI was found to be 14.765 and 8.094 mg g^{-1}, respectively. The relatively high adsorption capacity of the sorbents may be due to the fact that the chromate anions could be exchanged with the aniline counter ion. Moreover, higher adsorption capacity of MGO@PANI than Fe$_3$O$_4$@PANI may be attributed to the polymerization of both sides of the planar graphene oxide sheets, whereas Fe$_3$O$_4$@PANI is formed as the core shells. In addition, MGO is covered more conveniently by PANI due to high attraction of the carbonaceous structures via π-cation and π–π electronic interactions.

Effects of co-existing ions

The effect of common co-existing ions on the adsorption of Cr(VI) by MGO@PANI was studied. For this purpose, the procedure was performed in the presence of ions which usually accompany with the target analyte in real samples. An ion which caused a variation of more than $\pm 5\%$ in the recovery of Cr(VI) was considered as an interfering species. Based on the results, the 1000-fold excess of Na$^+$, K$^+$, Ca^{2+}, Mg^{2+}, Fe^{3+} and Al^{3+} ions showed no significant effects in the extraction efficiency. Since the sorption mechanism is anion exchange, it was predictable that cations have no significant effect in the extraction efficiency of Cr(VI). Also, 1000-fold excess of Cl$^-$ and 500-fold excess of NO$_3^-$, PO$_4^{3-}$ and SO$_4^{2-}$ had no obvious influences on the extraction under the optimized conditions.

Application to water samples

The analytical procedure was validated by analyzing the standard reference material (SRM 2109, NIST) for Cr(VI) speciation. For this purpose, 100 μL of the SRM was transferred into a 1000-mL volumetric flask and diluted with ultrapure water to the mark to obtain a concentration of 100 ng L^{-1}. The resulted concentration for Cr(VI) by the proposed method was 97.8 $\pm$ 1.63 ng L^{-1}, indicating good agreement between the obtained value and the certified value. In addition, to investigate the applicability of the proposed method in real samples, several water samples were collected and analyzed (Table 6). Except tap water, all other samples were filtered through cellulose acetate membrane filters (pore size 0.45 μm) prior to analysis. The tanner waste water was diluted 150 times, in order to be in the linear range of the proposed DMSPE–GFAAS method. Then, the pH of each sample was adjusted to 5.6 and subjected to the extraction procedure. Results are summarized in Table 6. To determine the method accuracy, each sample was spiked with appropriate amounts of Cr(VI) and the extraction procedure was carried out to calculate relative recoveries (RR%) using the following equation:

$$RR\% = \frac{C_{\text{found}} - C_{\text{real}}}{C_{\text{added}}} \times 100 \tag{4}$$

where C_{found}, C_{real} and C_{added} are the concentrations (ng L^{-1}) of analyte after adding a known amount of standard in the real sample, the initial concentration of analyte in the real sample and the concentration of a known amount of the standard which is spiked in the real sample. The obtained RR% values by three-replicate analyses of each sample were in the range of 100–110% elucidating acceptable accuracies of the proposed DMSPE–GFAAS method for subtrace determination of Cr(VI).

Conclusion

In this work, MGO@PANI was synthesized via a simple one-step procedure. The synthesized sorbent was characterized by SEM, FT-IR and EDX. The MGO@PANI was employed as an efficient anion-exchange sorbent for the dispersive magnetic solid-phase extraction of Cr(VI) in

aqueous samples. An orthogonal central composite design was used to optimize the effective factors on both adsorption and desorption steps. The results showed that the synthesized nanostructured sorbent has a great potential for subtrace determination of Cr(VI). High selective extraction of Cr(VI) at the presence of different interfering metal ions was provided by MGO@PANI due to extraction by the anion-exchange mechanism. Simple operation, low cost, low solvent consumption, relatively low required extraction time, good accuracy and precision, low LOD, high preconcentration factor and high adsorption capacity are the other advantages of the proposed method. Consequently, MGO@PANI can be used as a suitable alternative for extraction and determination of trace levels of Cr(VI) in environmental water samples.

References

1. H.M. Abu-Shawish, S.M. Saadeh, K. Hartani, H.M. Dalloul, J. Iran. Chem. Soc. **6**, 729 (2009)
2. B. Dhal, H.N. Thatoi, N.N. Das, B.D. Pandey, J. Hazard. Mater. **250**, 272 (2013)
3. P. Mamatha, G. Venkateswarlu, A.V.N. Swamy, A.C. Sahayam, Anal. Methods **6**, 9653 (2014)
4. B. Leśniewska, L. Trzonkowska, E. Zambrzycka, B. Godlewska-Żyłkiewicz, Anal. Methods **7**, 1517 (2015)
5. T.J. O'Brien, S. Ceryak, S.R. Patierno, Mutat. Res. Fundam. Mol. Mech. **533**, 3 (2003)
6. R. Karosi, K. Boruzs, Á. Béni, J. Posta, J. Balogh, V. Andruch, Anal. Methods **4**, 2361 (2012)
7. T. Sumida, T. Ikenoue, K. Hamada, A. Sabarudin, M. Oshima, S. Motomizu, Talanta **68**, 388 (2005)
8. D. Zou, Y. Qing, Y. Li, M. Liu, Y. Yang, J. Iran. Chem. Soc. **11**, 415 (2014)
9. D. Singh, R. Bharadwaj, B. Srivastava, A. Sahu, J. Sci. Ind. Res. **61**, 538 (2002)
10. S. Sadeghi, A.Z. Moghaddam, J. Iran. Chem. Soc. **13**, 117 (2016)
11. H. Chen, P. Du, J. Chen, S. Hu, S. Li, H. Liu, Talanta **81**, 176 (2010)
12. I. López-García, Y. Vicente-Martínez, M. Hernández-Córdoba, J. Anal. At. Spectrom. **27**, 874 (2012)
13. T. Madrakian, A. Afkhami, N. Rezvani-jalal, M. Ahmadi, J. Iran. Chem. Soc. **11**, 489 (2014)
14. H.W. Sun, W.J. Kang, J. Ha, S.X. Liang, S.G. Shen, J. Iran. Chem. Soc. **1**, 40 (2004)
15. A. Afkhami, S. Aghajani, M. Mohseni, T. Madrakian, J. Iran. Chem. Soc. **12**, 2007 (2015)
16. M. Soylak, A. Aydin, J. Iran. Chem. Soc. **9**, 263 (2012)
17. K.H. Shah, S. Mustafa, M. Waseem, A. Naeem, J. Iran. Chem. Soc. **9**, 895 (2012)
18. J.S. Suleiman, B. Hu, H. Peng, C. Huang, Talanta **77**, 1579 (2009)
19. D.M. Sarno, S.K. Manohar, A.G. MacDiarmid, Synth. Met. **148**, 237 (2005)
20. S. Ebrahim, A. Shokry, H. Ibrahim, M. Soliman, J. Polym. Res. **23**, 1 (2016)
21. T.M. Rettberg, J. Res. Natl. Bur. Stand. **93**, 450 (1988)
22. D.C. Marcano, D.V. Kosynkin, J.M. Berlin, A. Sinitskii, Z. Sun, A. Slesarev, L.B. Alemany, W. Lu, J.M. Tour, ACS Nano **4**, 4806 (2010)
23. https://en.wikipedia.org/wiki/Chromate_and_dichromate
24. N. Kamakura, T. Inui, M. Kitano, T. Nakamura, Spectrochim. Acta B **93**, 28 (2014)
25. K.M. Diniz, C.R.T. Tarley, Microchem. J. **123**, 185 (2015)
26. H. Tavallali, G. Deilamy-Rad, P. Peykarimah, Environ. Monit. Assess. **185**, 7723 (2013)
27. M. Rezvani, A.A. Asgharinezhad, H. Ebrahimzadeh, N. Shekari, Microchim. Acta **181**, 1887 (2014)
28. S.K. Behzad, M.M. Amini, A. Balati, M. Ghanbari, O. Sadeghi, J. Sol-Gel Sci. Technol. **78**, 446 (2016)
29. M. Karimi, A.M.H. Shabani, S. Dadfarnia, J. Braz. Chem. Soc. **27**, 144 (2016)
30. C. Cui, M. He, B. Chen, B. Hu, Anal. Methods **6**, 8577 (2014)
31. H.M. Jiang, T. Yang, Y.H. Wang, H.Z. Lian, X. Hu, Talanta **116**, 361 (2013)
32. X.P. Yao, Z.J. Fu, Y.G. Zhao, L. Wang, L.Y. Fang, H.Y. Shen, Talanta **97**, 124 (2012)
33. Y.F. Huang, Y. Li, Y. Jiang, X.P. Yan, J. Anal. At. Spectrom. **25**, 1467 (2010)
34. M. Faraji, Y. Yamini, A. Saleh, M. Rezaee, M. Ghambarian, R. Hassani, Anal. Chim. Acta **659**, 172 (2010)